

# We are IntechOpen, the world's leading publisher of Open Access books Built by scientists, for scientists

6,900

Open access books available

186,000

International authors and editors

200M

Downloads

Our authors are among the

154

Countries delivered to

TOP 1%

most cited scientists

12.2%

Contributors from top 500 universities



WEB OF SCIENCE™

Selection of our books indexed in the Book Citation Index  
in Web of Science™ Core Collection (BKCI)

Interested in publishing with us?  
Contact [book.department@intechopen.com](mailto:book.department@intechopen.com)

Numbers displayed above are based on latest data collected.  
For more information visit [www.intechopen.com](http://www.intechopen.com)



---

# Graphene Derivatives: Controlled Properties, Nanocomposites, and Energy Harvesting Applications

---

Ulises Antonio Méndez Romero,  
Miguel Ángel Velasco Soto, Liliana Licea Jiménez,  
Jaime Álvarez Quintana and  
Sergio Alfonso Pérez García

Additional information is available at the end of the chapter

<http://dx.doi.org/10.5772/67474>

---

## Abstract

Graphene is a ground-breaking two-dimensional (2D) material that possesses outstanding electrical, optical, thermal, and mechanical properties and that promises a new generation of devices. Despite all these, some applications require graphene-based materials with different characteristics, such as good solubility in organic solvents and a specific band gap to be dispersible in polymer nanocomposite matrix and applied as active layer, electron transport layer (ETL) or hole transport layer (HTL) in organic photovoltaics. Chemically modified graphene derivatives are studied, searching for better dispersions and even more properties for different applications. Most of the attention has been drawn to dispersions of graphene oxides or highly reduced graphene oxides. Therefore, this allows an opportunity to study the characteristics of materials with intermediate oxidation degrees and its applications.

**Keywords:** graphene oxide, reduced graphene oxide, band gap modification, OPVs, reduced graphene oxide functionalized

---

## 1. Introduction

Graphene, a unique two-dimensional carbon material with exceptional properties as high electrical and thermal conductivity, zero band gap, high optical transmittance and superior mechanical performance than steel [1], is often regarded as the material of the twenty-first century. A great focus is being added to graphene in all scientific fields, such as physics, chemistry, and even medicine. Nanocomposites, dispersions, and films that include graphene

in a polymer matrix are the trending topic of recent research studies. With graphene science on the growth, more investigation lines are getting opened, such as graphene synthesis and modification.

Certain applications require some characteristics that even graphene, with all its properties, cannot provide. This is the main reason for the continuous search for chemical modifications to graphene: graphene derivatives, which have an important role to play in recent research. It is a well-known fact that graphene oxide (GO) is one of the most studied derivatives. GO is graphene with carbon-oxygen bonds and has functionalities such as hydroxyl, carbonyl, and carboxyl groups (**Figure 1**). Therefore, GO is a highly hydrophilic molecule and, more important for electronics and energy-harvesting applications, this process provides a band gap ( $E_g$ ). For example, the energy difference between the highest occupied molecular orbital (HOMO) and the lowest unoccupied molecular orbital (LUMO) in the resulting complete oxidized material is around 3 eV [2], which is also directly related to the carbon-oxygen ratio [3]. Oxidation reactions include strong acid attacks with  $\text{H}_2\text{SO}_4$ ,  $\text{HNO}_3$ ,  $\text{H}_2\text{O}_2$ ,  $\text{KMnO}_4$ , or a mixture of them, being one of the most used by the Hummers method [4].

Most of the methods for quantification of carbon-oxygen functional groups include Boehm's titration [6], which uses different basic solutions to react in sequence with carboxyl, carbonyl, and hydroxyl moieties. Another quantification method is X-ray photoelectron spectroscopy (XPS), which uses the area result from fitting the signals corresponding to the binding energy of the sample for different carbon peaks. XPS can be used also to quantify  $\text{sp}^2$  and  $\text{sp}^3$  domains.

One of the most interesting applications for this type of materials is organic photovoltaics (OPVs). In this chapter, various approaches are explored to develop materials with a possible application in OPVs, based on modified GO into the active layer. It is well known that GO has a band gap of 3.1 eV, which can be further modulated by chemical reduction reactions [2]. The

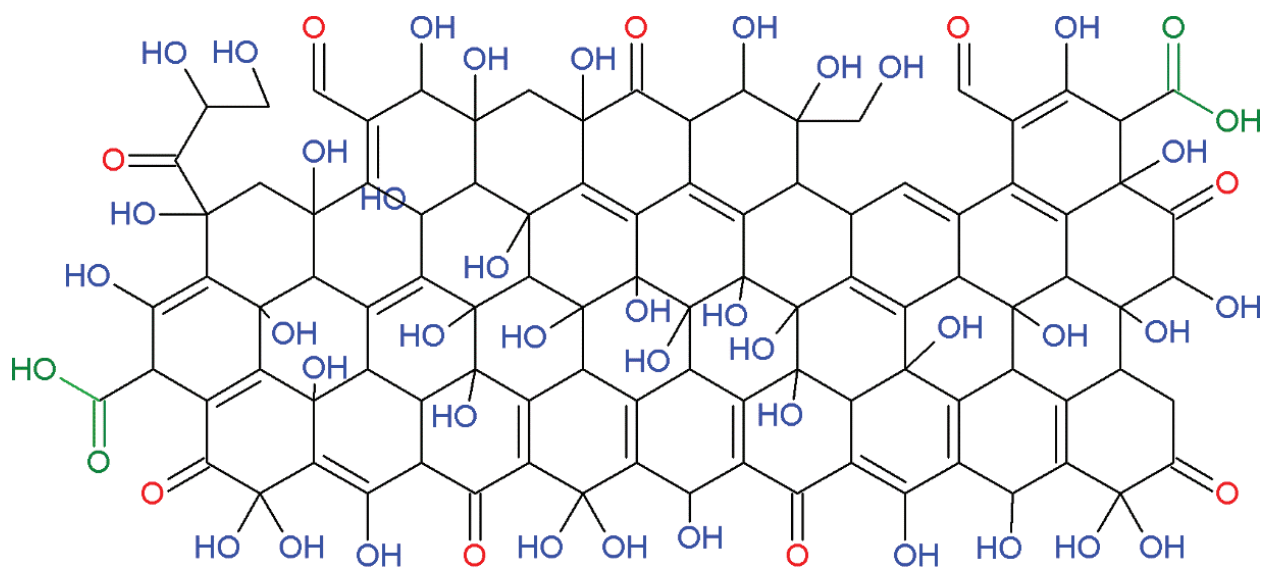


**Figure 1.** Graphene oxide structure in Lerf-klinowksy Model and different C-O functionalities. Hydroxyl in blue, carbonyl in red, and carboxyl in green [5].

reduction process can be carried out by innocuous agents, such as fructose, glucose, ascorbic acid, or ascorbic acid-6-palmitate, obtaining band gaps around 1.1 eV.

In recent years, alternatives have been explored with organic compounds (i.e., OPVs, also known as excitonic cells [7]), which have a great number of advantages compared with traditional silicon photovoltaics. Some of the main advantages are a lower weight, flexibility, simple mass production, and low cost. On the other hand, the OPVs have the limitation of low power conversion efficiency (PCE), compared to silicon based solar cells, with a maximum of 11% [8, 9], offering a big opportunity area for improvement. The PCE is the ratio between the maximum power in watts produced by the cell ( $P_{\max}$ ), divided by the power in watts of the incident light ( $\phi_e$ ) cf. Eq. (1).

$$PCE = \frac{P_{\max}}{\phi_e} \quad (1)$$

The most efficient OPVs are based on the concept of bulk heterojunction (BHJ) [10]. In this type of solar cell, presented in **Figure 2**, where electron donor material (usually polymer) is mixed with an electron-accepting material (derived from fullerenes in most cases) in an organic solvent (1,2-dichlorobenzene, oDCB, for example) and subsequently deposited by spin coating on an indium-tin oxide (ITO) layer previously deposited on a glass or PET substrate. During evaporation of the solvent and subsequent treatments, an interconnected bicontinuous microphase is generated, which creates a large interfacial area between the donor material and the acceptor material (i.e., the BHJ), also called photoactive layer or simply active layer. The next layer deposited is lithium fluoride (LiF), which prevents the transportation of the holes, followed by a metal electrode (aluminum for example). These two layers are deposited by sputtering, inside a glove box in atmosphere of  $N_2$  [11].

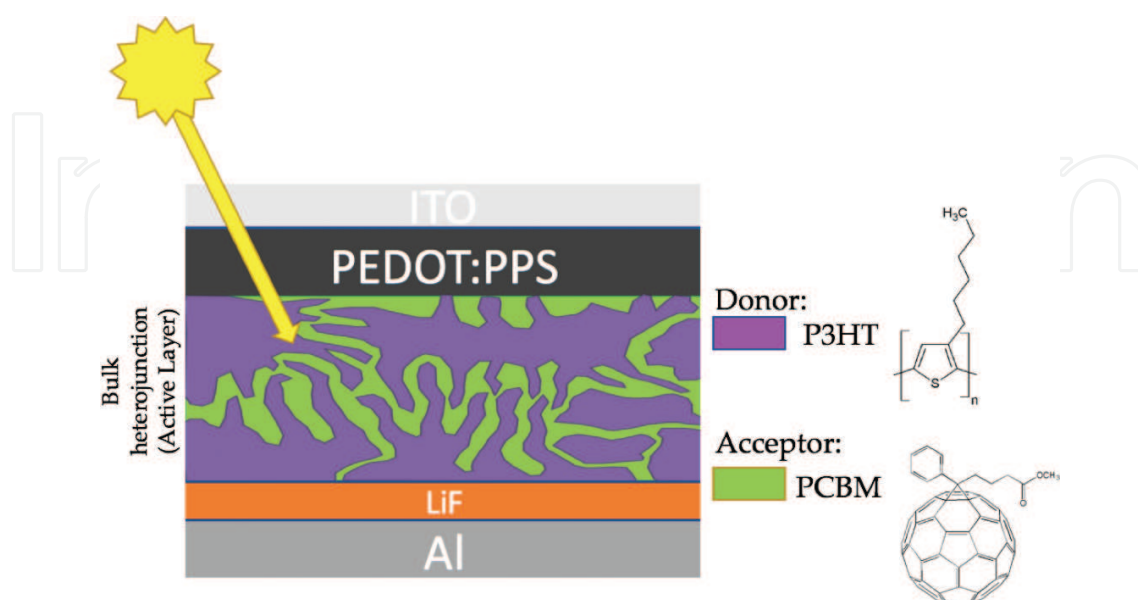


**Figure 2.** Typical diagram of an OPV-BHJ [12].

The heterojunction is important because of the large donor-acceptor interface that is created since it is precisely there, where the separation of charges takes place.

Another parameter used to describe OPVs is the external quantum efficiency (EQE), which is a parameter that indicates the ratio of the photogenerated electrons related to the incident photons. This depends on five factors: absorption of the light ( $\eta_A$ ), diffusion of exciton ( $\eta_{\text{diff}}$ ), dissociation of exciton ( $\eta_{\text{diss}}$ ), transport of charges through films ( $\eta_{\text{tr}}$ ), and charge collection on electrodes ( $\eta_{\text{cc}}$ ) [13]. The equation of quantum efficiency is given below:

$$EQE = \eta_A \eta_{\text{diff}} \eta_{\text{diss}} \eta_{\text{tr}} \eta_{\text{cc}} \quad (2)$$

Finally, the fill factor (FF) is another term that characterizes the device and defines the efficiency of a cell and is given in Eq. (3).

$$FF = \frac{J_{sc} V_{oc}}{\phi_e} = \frac{J_m V_m}{J_{sc} V_{oc}} \quad (3)$$

Where  $J_{sc}$  is the short circuit current density,  $V_{oc}$  is the open circuit voltage, and  $J_m$  and  $V_m$  are the maximum current and voltage, respectively. These values are obtained by an electrical characterization of the device, using typical curves of current against voltage, through two measurements, one in darkness and the other under illumination.

The common feature of the materials used in the active layer of the OPVs is that they are small molecules or polymers with conjugated bonds (i.e., carbon-carbon bonds in alternating  $sp^2$  hybridization), allowing the continuous transportation of electrons along the molecular structure. In addition, these materials must have adequate values of HOMO, LUMO, and  $E_g$ . Some examples of these materials are poly(3-hexylthiophene) (P3HT), [6,6]-phenyl C61 butyric acid methyl ester (PCBM), or [6,6]-phenyl C71 butyric acid methyl ester (PC<sub>71</sub>BM).

A further aspect to consider is the solubility of graphene oxide in organic solvents, normally used for manufacturing OPVs such as 1,2-dichlorobenzene, chloroform, or toluene.

## 2. Graphene oxide

Graphene oxide (GO) is a molecule of graphene with oxygen functional groups (carbonyl, hydroxyl, epoxy, and carboxyl), synthesized from graphite, either by the method of Brodie, Staudenmaier, or Hummers [4, 14, 15] (structure as shown in **Figure 1**). GO has an  $E_g$  related to the stoichiometric ratio between carbon and oxygen, resulting in a zero band gap (0% oxygen) around 3 eV for graphene oxide with a proportion of 50% oxygen, according to the computational calculations reported elsewhere [3]. **Figure 3** shows the chemical reaction in Hummers method.

It is important to mention that **Figure 3** corresponds to the synthesis of graphite oxide, which is a bright yellow dispersion that needs a multiple step washing with DI H<sub>2</sub>O in centrifuge and

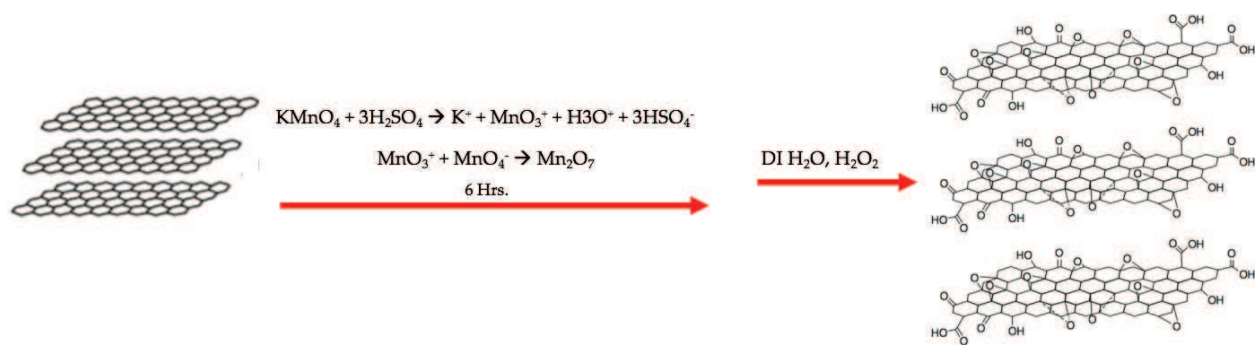


**Figure 3.** Chemical oxidation in Hummers' method [4].

exfoliation in ultrasonic bath in order to obtain the graphene oxide. The latter is a brown-reddish dispersion with a characteristic UV-vis spectrum, with  $\pi \rightarrow \pi^*$  and  $n \rightarrow \pi^*$  transitions for C—C and C=O bonding, respectively, shown in **Figure 4** [2].

A more detailed analysis of the GO is performed with XPS for C1s, presented in **Figure 5**, in order to determine the contribution for C=C bonding and C=O, which is 40 and 60%, respectively, for GO after 6 hours of oxidation in the presented Hummers reaction. This technique allows to specify the C=C and C—C, which is 21.3% and 18.73%. Also for the C=O=C and C=OH is 52.03%, C—O is 3.54%, and for COOH 4.4% [2].

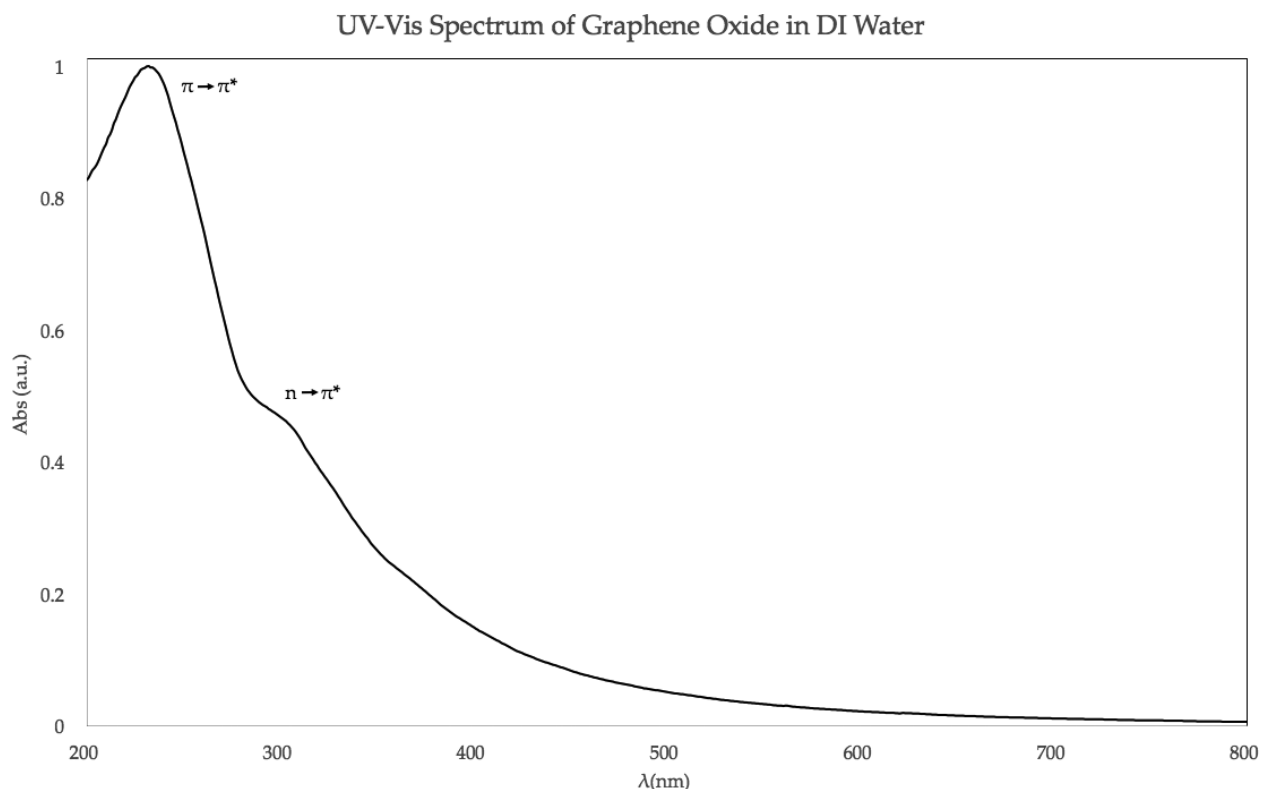


**Figure 4.** UV-vis spectrum of graphene oxide dispersion in DI H<sub>2</sub>O [12].



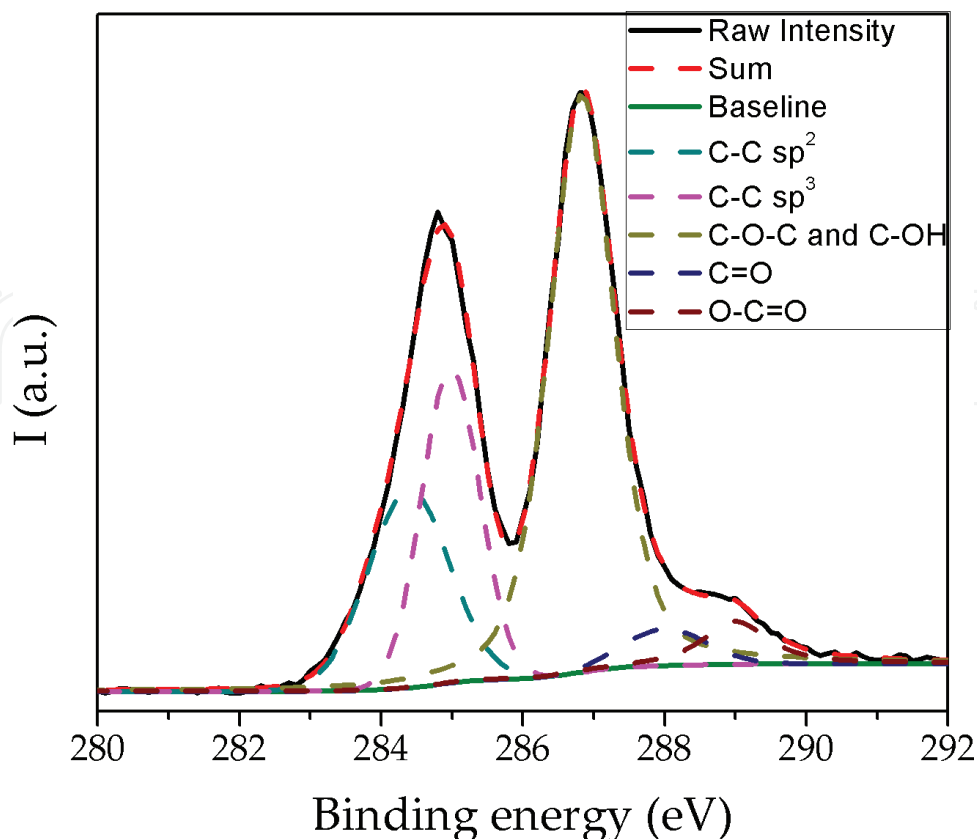


Figure 5. XPS for C1s [2].

### 3. Reduced graphene oxide

To apply these graphene-based materials, additional processes are required to obtain a material that meets the required characteristics. Graphite, as previously discussed in this chapter, must be oxidized (GO) in order to obtain a band gap. However, this molecule is extremely hydrophilic and therefore insoluble in organic solvents commonly used in OPVs, such as oDCB, toluene, and chloroform.

Nevertheless, the resulting  $E_g$  is too high—as we mentioned before—but because its relation with the percentage of oxygen, a common strategy used to modify that value consists in the chemical reduction (i.e., removing the oxygen atoms), obtaining values of 2.7–0.1 eV, when hydrazine is used. However, due its toxicity, it is also preferable to use harmless reducing agents such as fructose, glucose, and ascorbic acid in basic medium, obtaining values of 2.7–1.1 eV [2, 16]. The XPS analysis, plays a key role for the oxygen quantification, is shown in Figure 6.

To determine the real contribution of the mentioned reducing agents, an experiment with only  $\text{NH}_4\text{OH}$  was carried out, and an increase of up to 35% in  $\text{sp}^2$  domains was observed. However, the contribution of carbonyl and carboxyl had a low modification, as seen in Table 1, demonstrating that  $\text{NH}_4\text{OH}$  alone is not able to decrease the most oxidized states of carbon. A

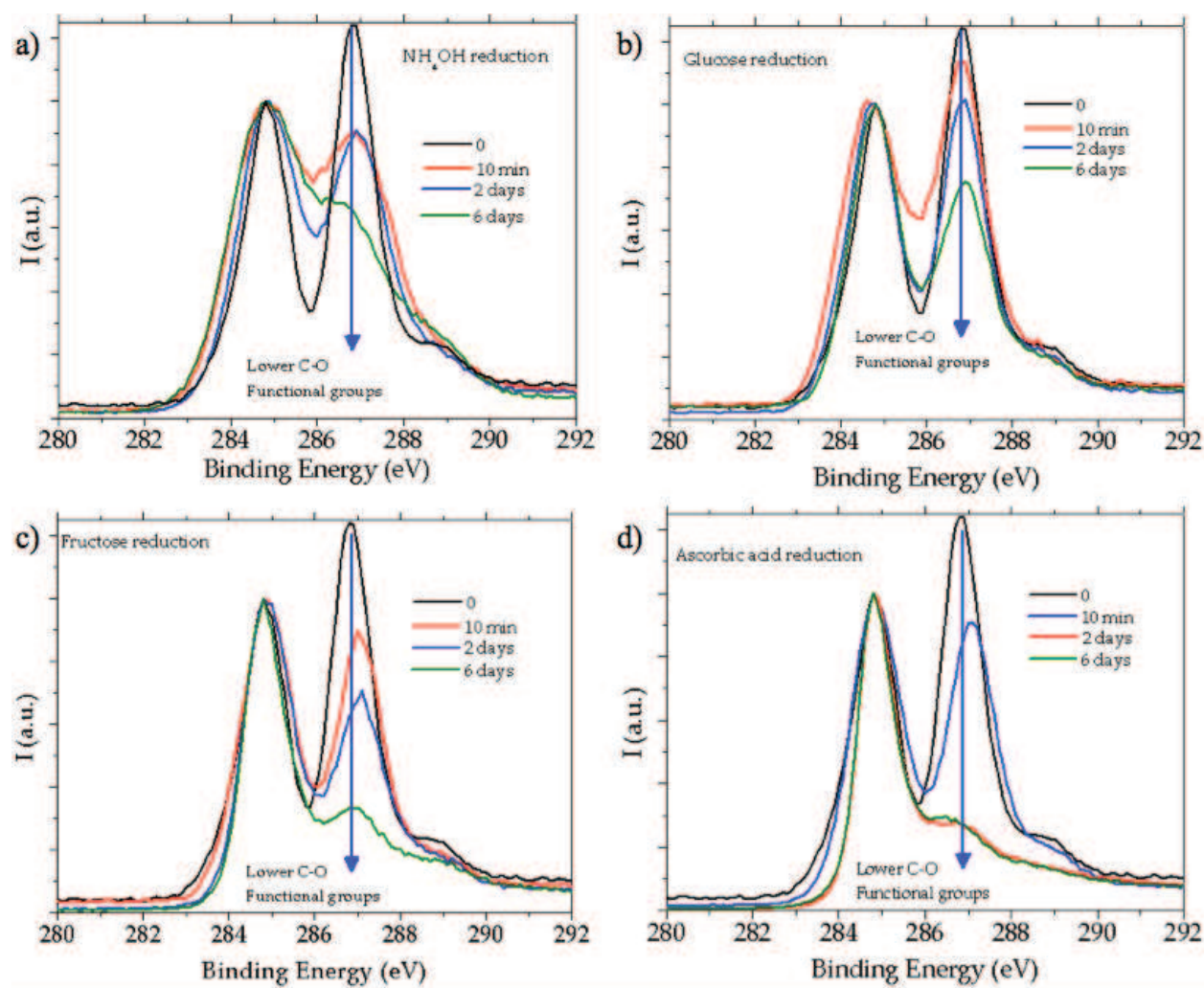


**Figure 6.** XPS C1s spectra for reduction with: a)  $\text{NH}_4\text{OH}$ ; b) glucose at pH 10; c) fructose at pH 10; and d) ascorbic acid at pH 10 after 10 min, 2 days, and 6 days [2].

comparable behavior is detected for the addition of glucose, where a similar result on the oxygen signal decrease can be observed (cf. **Figure 6b**).

Fructose reveals enhanced recovery of  $\text{sp}^2$  contribution to 41.3% after 6 days. Among all reagents investigated, ascorbic acid provides the best recovery capability of  $\text{sp}^2$  domains (~53% after 6 days) and elimination capability of epoxide and hydroxyl groups. A summary is presented in **Table 1** [2].

Time	C—C ( $\text{sp}^2$ )	C—C ( $\text{sp}^3$ )	C—O—C and C—OH	C=O	COOH
C1s contributions of GO after 6 hours of oxidation (%)					
0 min	18.73	21.30	52.03	3.54	4.40
Contributions after $\text{NH}_4\text{OH}$ reduction (%)					
10 min	30.66	30.07	28.56	6.95	3.77
2 days	34.88	21.85	32.21	5.80	5.26
6 days	35.30	27.50	22.04	7.47	7.69



Time	C—C (sp <sup>2</sup> )	C—C (sp <sup>3</sup> )	C—O—C and C—OH	C=O	COOH
C1s contributions after glucose reduction (%)					
10 min	31.79	25.40	34.25	5.67	2.89
2 days	30.64	19.14	39.54	5.92	4.76
6 days	37.06	20.71	30.52	5.92	5.80
C1s contributions after fructose reduction (%)					
10 min	32.67	21.57	36.56	5.13	4.07
2 days	34.37	23.69	33.51	2.19	6.25
6 days	41.31	19.99	20.71	1.62	16.38
C1s contributions after ascorbic acid reduction (%)					
10 min	30.38	21.02	35.02	7.59	5.99
2 days	51.03	17.86	9.85	6.46	14.81
6 days	53.03	16.11	12.14	7.03	11.69

Reprinted from Ref. [2].

**Table 1.** Area percentage of functional groups after reduction.

Graphene oxides resulting from chemical reductions (rGO) continue to exhibit low dispersibility in organic solvents, so it is necessary to functionalize them with long chain hydrocarbon molecules.

#### 4. Surface modification

The development of novel methods for surface modification of graphene is a challenge in the science and technology of nanocomposite materials. The functionalization of graphene derivatives should provide good stability and is necessary to improve their dispersion in any polymeric matrix. Therefore, many physical and chemical properties in nanocomposites obtained could be improved. The chapter aims to present the recent research advances in new methods of solution processable graphene derivatives, chemical modification, properties, and their incorporation in nanocomposites materials for applications in energy harvesting.

Graphene oxide has dispersion difficulties in nonpolar solvents due to its hydrophilic nature. A work [17] concerning the test of organic solvents for dispersion is the base for this analysis. The work suggests that the best solvents for this endeavor are those with high electrical dipole moment, including THF, ethylene glycol, and DMF. However, there are some exceptions for the dispersion and exfoliation of GO synthesized by Hummers method. One of these deviations from the rule is DMSO; in this solvent, dispersion was bad. The work is supported by photographs where sediments were visible on the bottom of the glass, making evident its bad dispersion.

In an unpublished work from our group, graphene oxide solubility with chlorinated solvents was studied, looking for the incorporation of graphene oxide to polymer solar cells to

determine the solubility of different GOs with variable degrees of oxidation. **Figure 6** shows the reduction of GO with reducing agents in basic media. Carbon-oxygen ratios calculated from XPS survey are shown in **Figure 7**.

The solubility tests are shown in **Figure 8**. The maximum solubility achieved with this reducing method was less than 2 mg/mL. The trend shows that a minimum 3.5 carbon/oxygen ratio is required to disperse partially reduced graphene oxide.

For practical applications, a solubility of 10 mg/mL of electron acceptor is required; therefore, to increase solubility, surface modifications are required.

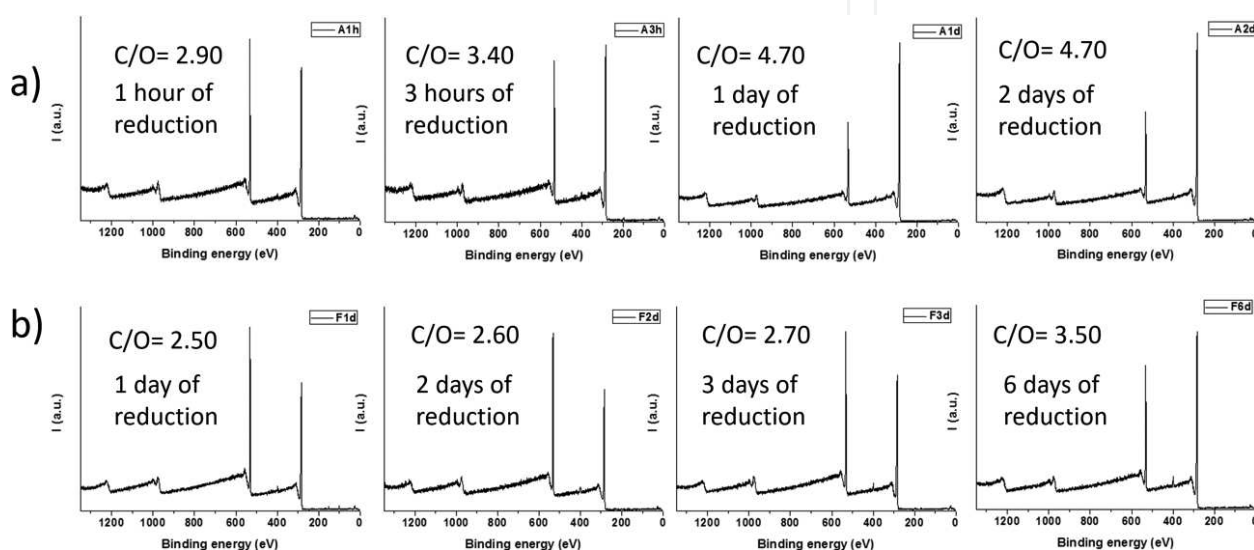


**Figure 7.** XPS survey of (a) GO with variable degrees of oxidation reduced with fructose; (b) reduced with ascorbic.

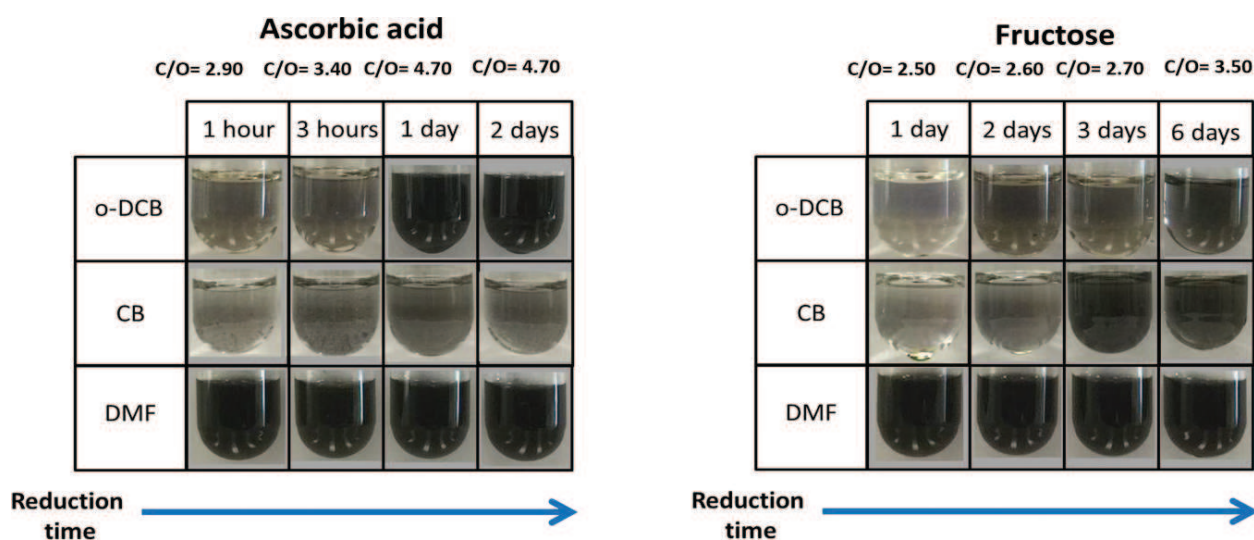


**Figure 8.** Dispersions of reduced GO with ascorbic acid and fructose in o-dichlorobenzene (o-DCB), chlorobenzene (CB) and dimethylformamide (DMF). For o-DCB 3.5 C/O ratio is required to have a good dispersion.

Graphene oxide is a family of decorated graphene structure with oxygen moieties that can be further functionalized with different polymer chains. Most reported functionalizations exploit the carboxylic endings for anchoring long alkyl chains through esterification or amidation.

Noncovalent functionalization can work via electrostatic interactions or  $\pi$ - $\pi$  interactions, between the functionalizing agent and the graphene. This kind of functionalization is preferred

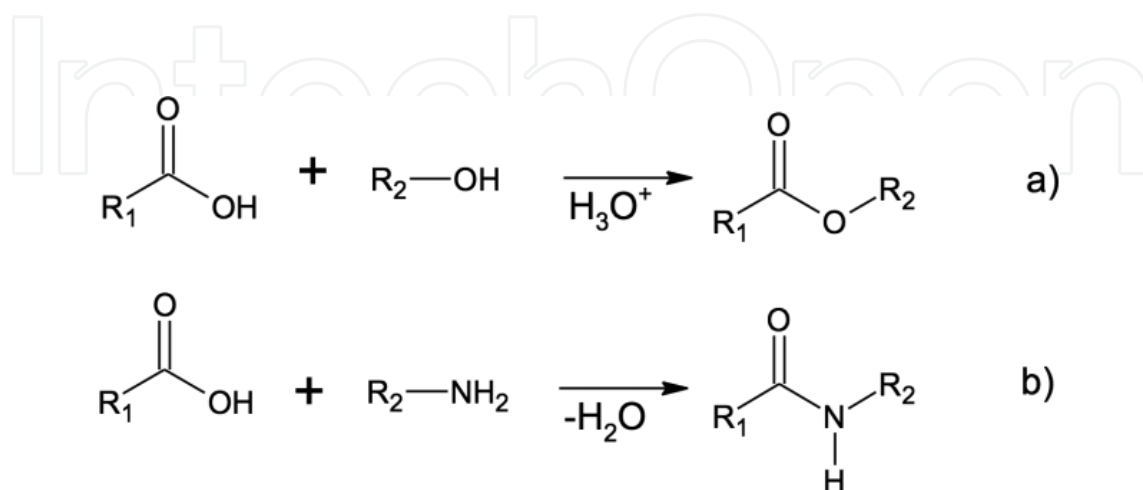


Figure 9. (a) Esterification reaction and (b) amidation reaction [5, 20].

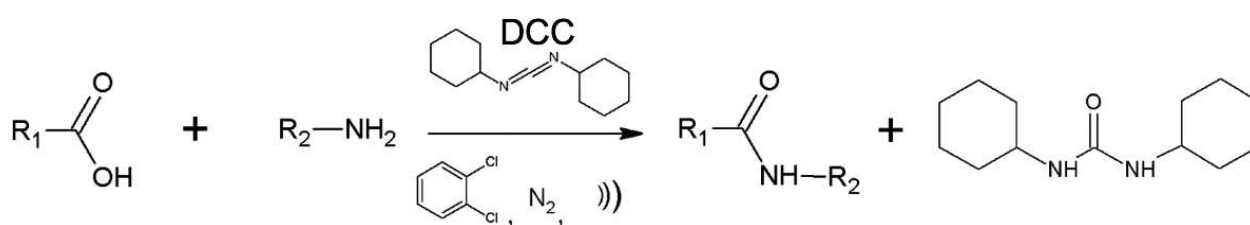


Figure 10. Amidation of a carboxylic acid using DCC in  $N_2$  atmosphere [12].

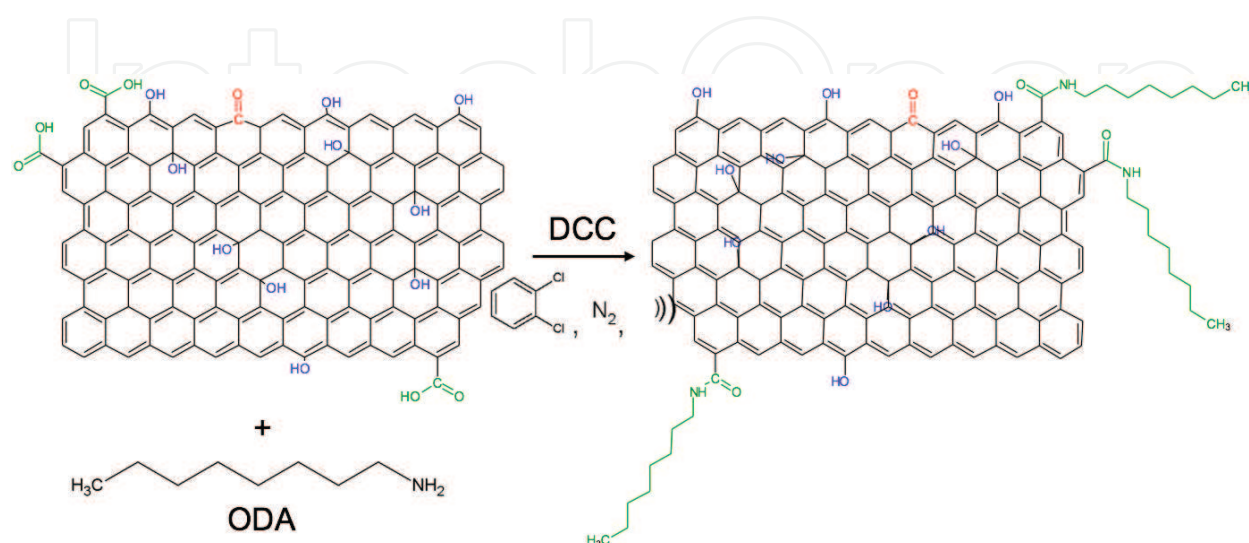
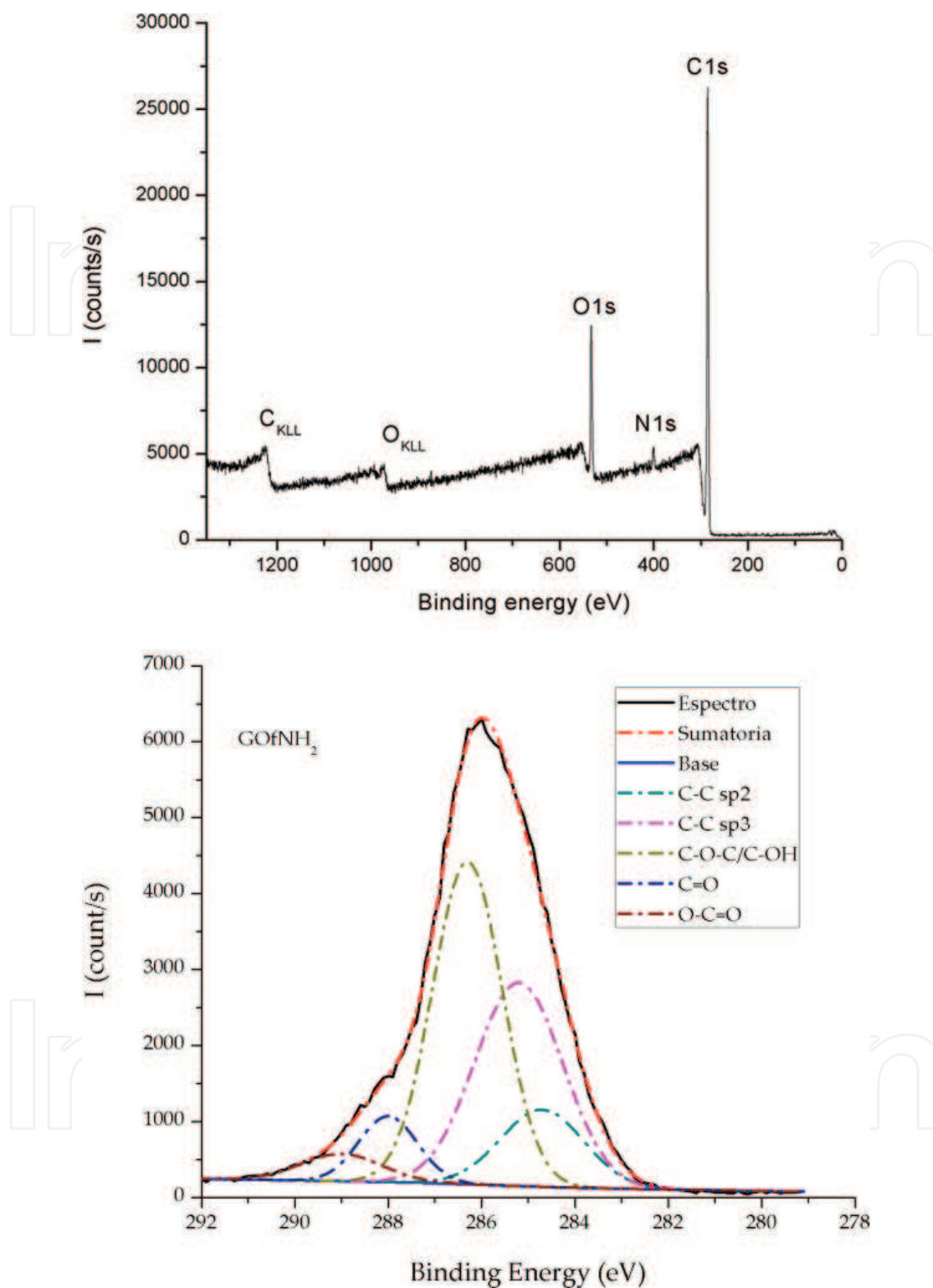


Figure 11. Surface modification of reduced graphene oxide with octadecylamine [12].



**Figure 12.** XPS survey and High resolution  $C1s$  of reduced graphene oxide functionalized with ODA [12].

for applications in which optical or electronic properties are critical. A disadvantage is the difficulty of removing the dispersant agent from the graphene surface due to high stability between them [18, 19].

Covalent functionalization is based on direct chemical reactions over functional groups of graphene oxide. The first step of the reaction will be referred as later proposed classification of graphene, because its similarities on reactions between carbon nanotubes (CNTs). These reactions are referred as first-generation (1G) modifications. They have the characteristic of introducing a functional group by covalently bonding to a carbon atom; frequently these reactions include strong oxidations.

Another kind of modification is the consecutive reaction of the already introduced 1G functional groups. Typically the reactions include esterifications and amidations, which appear in **Figure 9**. This is useful, not only for dispersing nanoparticles in solvent media but also for conferring affinity for polymer matrices because interactions between dispersant agent and the matrix occur. These reactions are referred as second-generation (2G) modifications.

However, the above representation is just a simplified way, as unusual it might seem. In order to carry out a successful amidation, a catalyst is often used, as dicyclohexylcarbodiimide, as shown in **Figure 10**.

With this procedure, it is possible to use the carboxylic acids at the edge of the reduced graphene oxide to make a surface modification not only to improve the solubility, but also to prevent the restacking of the layers by the steric hindrance using a long chain alkylamine as octadecylamine (ODA), given the molecular structure shown in **Figure 11**.

This modification can be observed in the XPS analysis for the peak attributed to N1s is shown in **Figure 12**, which was not present before the functionalization.

## 5. Band gap modification

As previously mentioned, the band gap of GO is related to the carbon-oxygen ratio, which implies that removing the number of oxygen present in the molecule leads to a band gap decrease. Moreover, gradual restoration of graphitic structure ( $sp^2$ ) with time offers the possibility of tuning the band gap in a controlled way. The XPS is an amazing tool to determine the content of oxygen on graphene materials. However, the easiest way to follow the changes in band gap through chemical reduction reactions is from UV-vis spectrums and then analyzed by Tauc plot. The information obtained by the spectrum is the absorbance of light at every wave length ( $A_\lambda$ ), which is related to the intensity of the incident light ( $I_0$ ) in a logarithmic way, as shown in Eq. (4).

$$A_\lambda = -\text{Log}_{10} \frac{I}{I_0} \quad (4)$$

It is a well-known fact that transmittance is the ratio between the intensity of the incident light ( $I_0$ ) and transmitted ( $I$ ), as described in Eq. (5). This is also related to the Lambert Beer's law and the absorption coefficient ( $\alpha$ ) and  $z$  is the optical path of the cell, usually equal of 1 cm.

$$T = \frac{I}{I_0} = e^{-\alpha z} \quad (5)$$

Which allows to relate the absorbance to transmittance as follow in Eq. (6) and finally, relate  $\alpha$  to  $T$  in Eq. (7).



$$T = 10^{-A_\lambda} \quad (6)$$

$$\alpha = -LnT \quad (7)$$

Finally, it is just needed to change the wavelength for energy ( $E$ ) in eV, with Eq. (8).

$$E = \frac{hc}{\lambda} \quad (8)$$

For example, from **Figure 4**, using these simple equations, it is possible to make the Tauc plot for GO as shown in **Figure 13**, where it is very easy to determine the band gap value.

The reduced graphene oxide with ascorbic acid, for 1 hour, 3 hours, 1 day, and 2 days at room temperature, [2] shown in **Figure 14**, presents the reduction in C-O contribution at 286.6 eV for C1s in XPS and the Tauc plot for each sample, making clear the band gap modification, in accordance to the oxygen decrease.

This applies for the other samples, such as the reduced graphene oxide with fructose, presented in **Figure 15**, with the same behavior: the reduction in the oxygen content is directly related to the band gap modification.

As expected, the surface modification shown in **Figure 11** also gives a band gap modification by the incorporation of different atoms to carbon in accordance to some computational results [21]. The value of this band gap modification for functionalization was obtained experimentally from the Tauc plot and is presented in **Figure 16**.

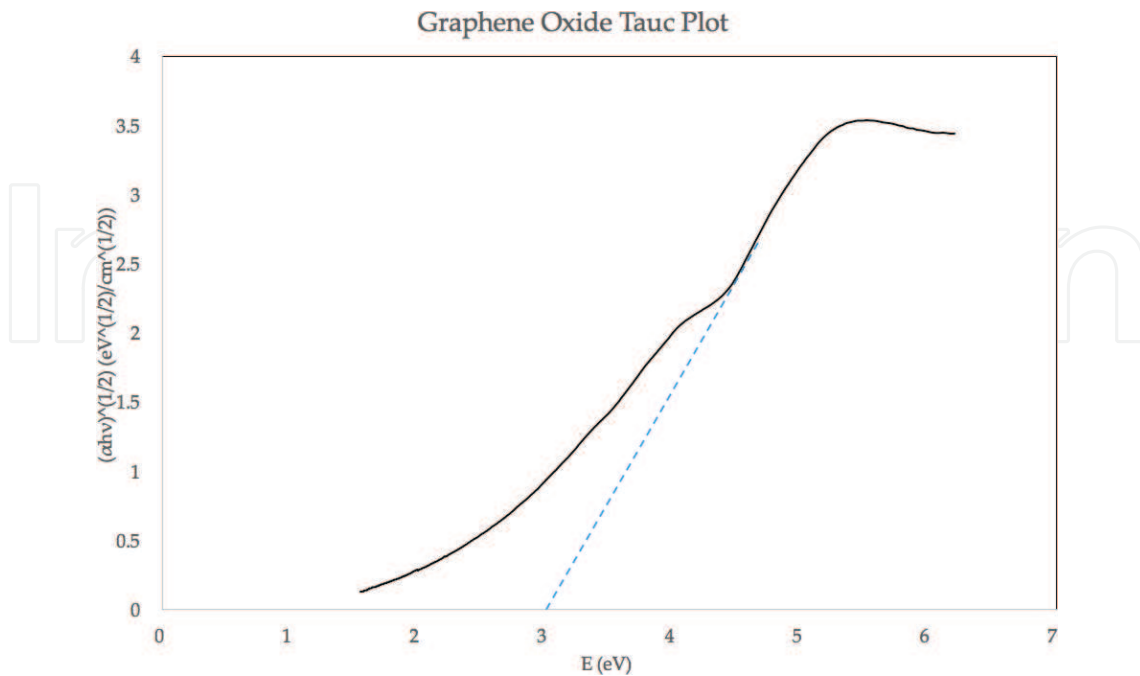


**Figure 13.** Tauc Plot for graphene oxide after 6 hours of oxidation [12].

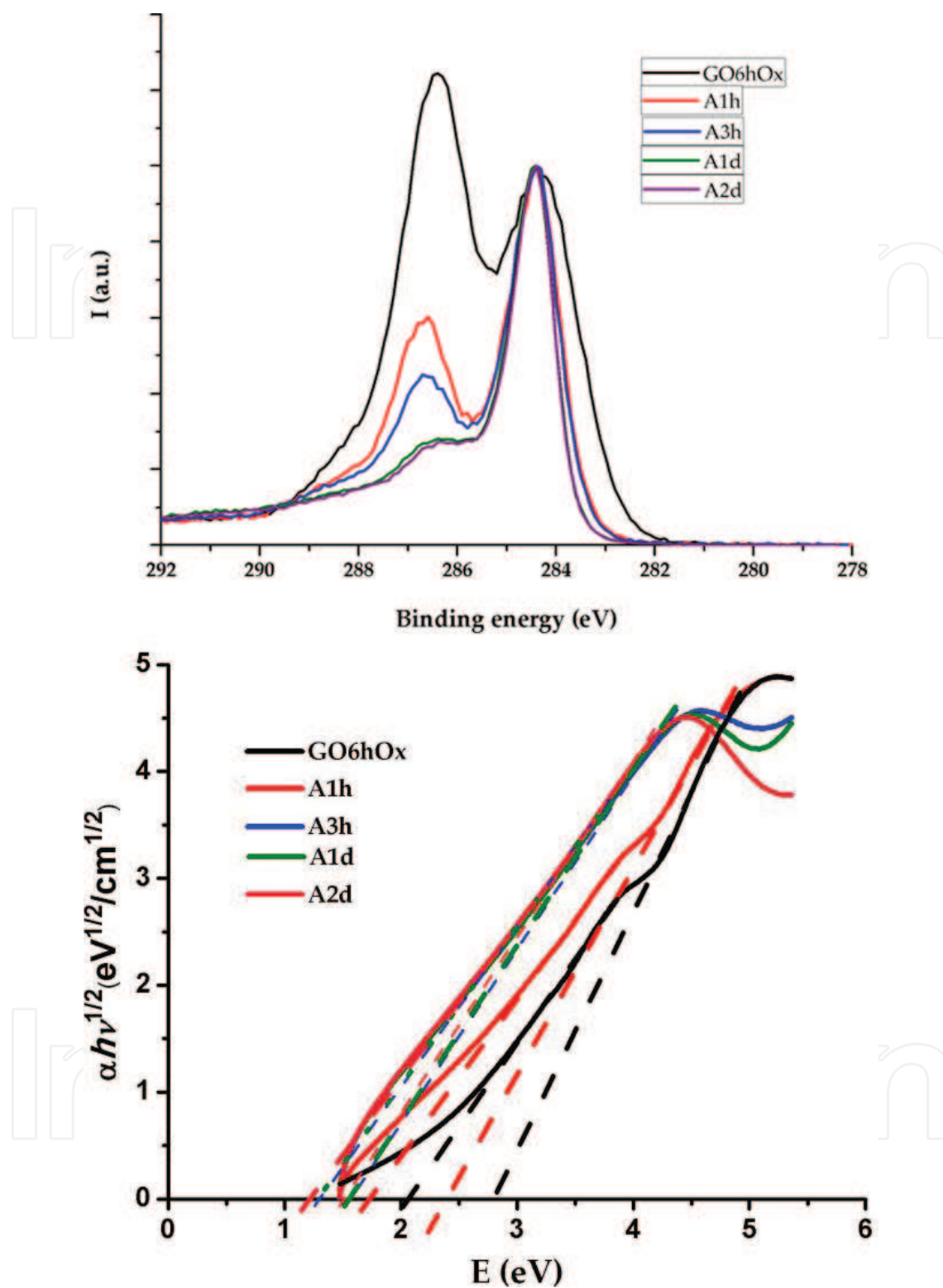


**Figure 14.** XPS C1s and Tauc plots for reduced graphene oxide with ascorbic acid. [2]

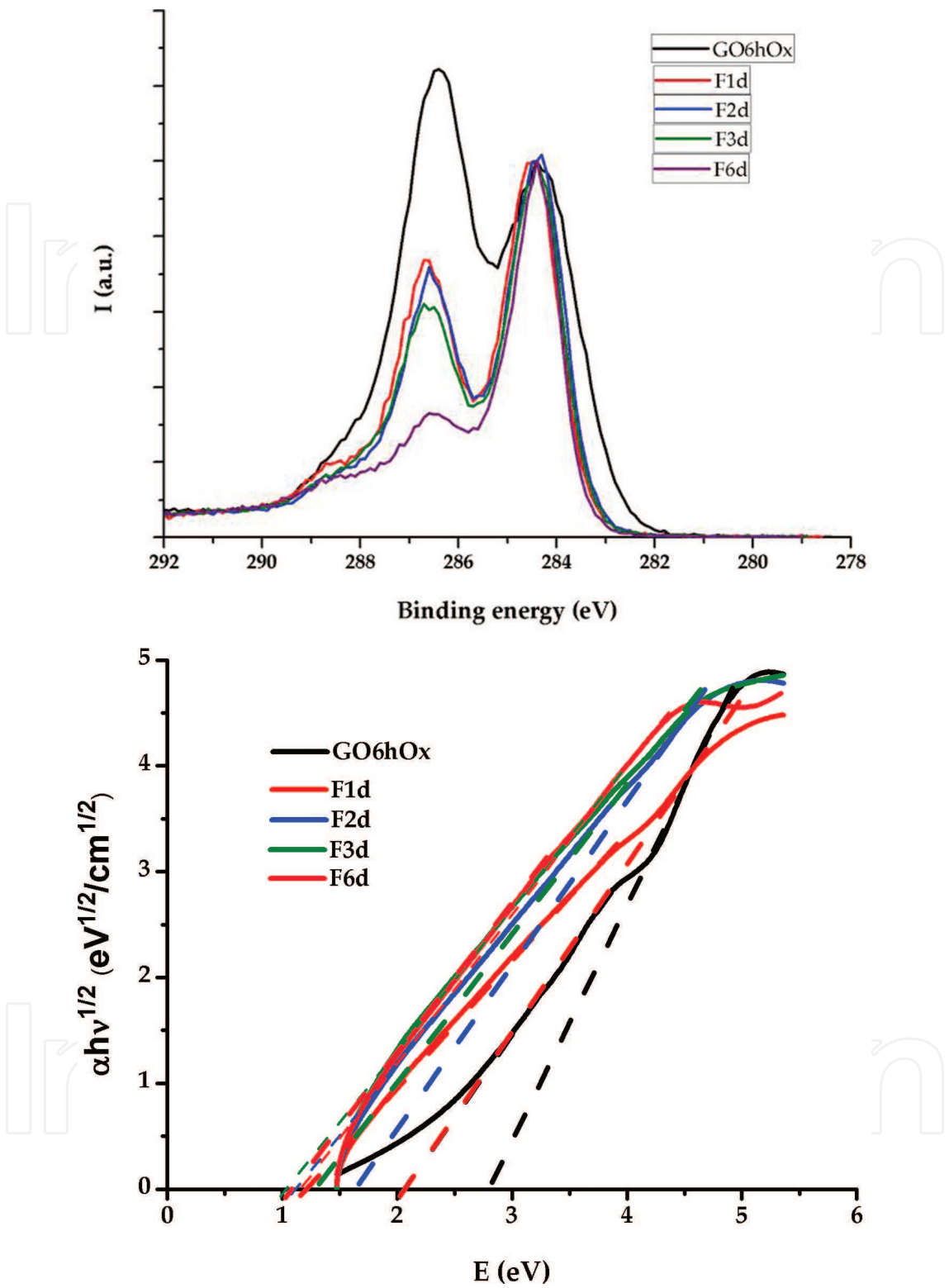


Figure 15. XPS C1s and Tauc plots for reduced graphene oxide with fructose. [2]

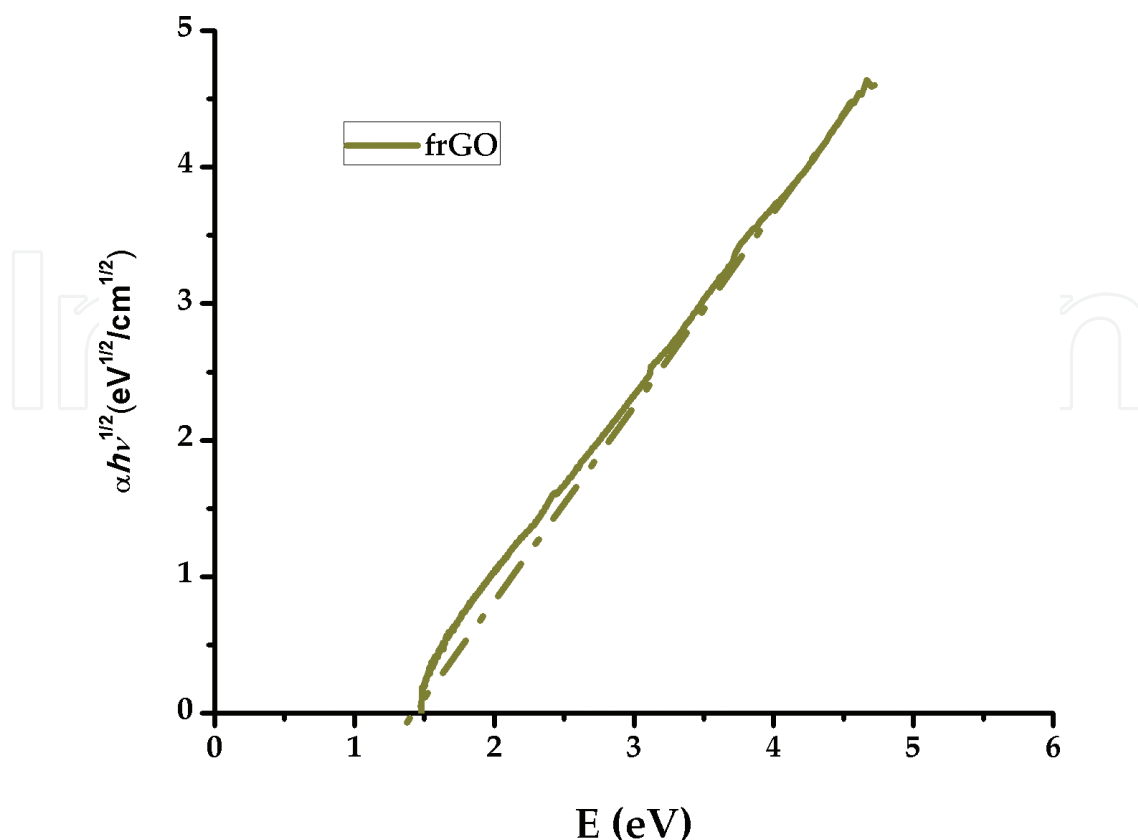


Figure 16. Band gap modification by surface modification of reduced graphene oxide [12].

## 6. Applications for energy harvesting devices

Energy harvesting is the process of capturing minute amounts of energy from one or more of these naturally occurring energy sources, accumulating them and storing them for further use. Graphene has the potential to address several scientific challenges, ranging from the need for more efficient alternative energy technologies. The unique properties of graphene previously mentioned along the present chapter shows the characteristics for energy-harvesting application, especially for its use in solar cells.

Since graphene monolayers were analyzed and obtained by micromechanical exfoliation in 2004 [22], graphene, as well as graphene oxide and reduced graphene oxide, has been added to the list of materials with potential application in OPVs in their different components, either in substitution of a previously used material or forming synergies that lead to an improvement in the devices. This is because of the three types of materials that have very different band gaps, from zero to 3 eV; HOMO values from  $-6.6$  to  $-4.8$  eV; LUMO values of  $-3.6$  to  $-4$  eV for GO and rGO; and Fermi level of  $-4.5$  eV for graphene [23].

Based on the previously described characteristics of the graphene, it is expected that the first applications designed for it are in [1] substitution of the indium-tin oxide (ITO) electrodes, since this material is fragile, expensive, and with a transmittance of 90% [1]. It has been

found that by replacing ITO with graphene, the efficiency of the device increases from 3.86 to 3.98% [24].

The main application of GO in OPVs, consists in the incorporation of this as a hole transport layer (HTL) between the active layer and the anode, replacing the PEDOT:PSS, achieving increases in the PCE of the order of 10% in a device with active layer of P3HT: PCBM [25, 26].

Moreover, it has been reported that incorporation of reduced and functionalized graphene oxide has successfully been carried out as an electron transport layer (ETL), between the active layer and the cathode, improving PCE by 15% for a device with a typical active layer of P3HT: PCBM [18, 27].

As expected, graphene and graphene oxide-based materials have also been used in the active layer of the OPVs, combined with P3HT: PCBM, obtaining a maximum PCE of 1.046% [28] or even without any polymer, only using PCBM/rGO/SWCNTs as active layer, obtaining a PCE of 1.3%, but with a significant improvement in thermal stability and resistance to aging by atmosphere with oxygen [29].

In addition, it has been reported that the incorporation of metallic nanoparticles in the organic photovoltaic devices leads to a significant increase in their efficiency. According to [30], the incorporation of reduced graphene oxide decorated with gold nanoparticles (rGO-AuNPs) instead of the typical PEDOT: PSS hollow conveyor layer, generates an increase of more than 25% in the efficiency of the device, this because the introduction of localized surface plasmon resonance (LSPR) generates a considerable increase in photocurrent. Following this trend, the incorporation of rGO-AgNPs into an active P3HT: PCBM blend layer, leads to a 24.7% increase in device efficiency, due to an increase in the photocurrent by the LSPR [31].

It has even been observed an increase of 116% in OPVs devices containing GO-AgNPs-PEDTO:PSS compared to those containing only GO-PEDOT:PSS as active layer [32].

## 7. Conclusion

The vast properties of graphene open endless possibilities for very different purposes. However, some applications require characteristics achieved through graphene derivatives such as graphene oxide, reduced graphene oxide, and reduced graphene oxide functionalized. Tailoring of the properties and surface chemistry of graphene lays on the control of its performance in a polymer matrix and a device.

Therefore, the capability of controlling these properties is of great importance. Moreover, a functionalization that makes reduced graphene oxide soluble in organic solvents must be successfully achieved, due to the varieties of applications and specific needs of the different energy harvesting devices' demands.

The chemical reduction of graphene oxide has been carried out by innocuous agents such as ascorbic acid, fructose, and glucose, controlling the band gap value of the resulting materials.



A process to decrease the band gap, by means, reducing the oxygen content in graphene oxide, i.e. rGO, was established. GO was synthesized through a modified Hummers method, and it has been found that  $\text{NH}_4\text{OH}$ , glucose, fructose, and ascorbic acid at pH 10 can be used to modify the band gap. The XPS C1s and UV-vis spectra indicate the gradual elimination of oxygen groups and restitution of graphitic structure, ensuing to a decreased value of band gap.

Ascorbic acid at pH 10 is more effective and fast for  $\text{sp}^2$  restitution, resulting in an optical band gap of 1.55 eV. The chemical reduction by fructose and glucose at pH 10 is slower which could be preferred in order to have a more precise control of band gap, but the total  $\text{sp}^2$  restoration is lower than that achieved by the ascorbic acid, nevertheless, it has the lowest band gap 1.15 eV with fructose at pH 10.

For application in organic solar cells, low band gaps are important because the PCE depends strongly on the effective generation, diffusion, and dissociation of the exciton. Because most of the solar energy is in the visible spectrum, a band gap in these values means more absorption of light and hence more exciton generation. Another aspect to consider is that restitution of  $\text{sp}^2$  domains entails a better exciton diffusion, because of the high carrier mobility. Finally, considering the band gap as the energy difference between the HOMO and LUMO, a low value is advantageous because the difference of the LUMOs, both in the acceptor and donor molecules or polymers, must be adequate for the exciton bonding dissociation and therefore increase the PCE.

## Acknowledgements

The authors are beholden for the technical support and facilities at CIMAV Monterrey, as well as to the Mexican National Research Council CONACyT for the scholarship of the students involved in this work. Lilia Magdalena Bautista Carrillo and Luis Gerardo Silva Vidaurri for UV-Vis spectra and XPS spectra, respectively, are also acknowledged.

## Author details

Ulises Antonio Méndez Romero<sup>1</sup>, Miguel Ángel Velasco Soto<sup>1</sup>, Liliana Licea Jiménez<sup>1,2</sup>, Jaime Álvarez Quintana<sup>1,2</sup> and Sergio Alfonso Pérez García<sup>1,2\*</sup>

\*Address all correspondence to: alfonso.perez@cimav.edu.mx

1 Center for Advanced Materials Research S.C. (CIMAV), Unidad Monterrey, Apodaca, NL, Mexico

2 GENES—Group of Embedded Nanomaterials for Energy Scavenging, Apodaca, NL, Mexico

## References

- [1] Garg, R., et al., Deposition methods of graphene as electrode material for organic solar cells. *Advanced Energy Materials*, 2016. 1601393. doi:10.1002/aenm.201601393
- [2] Velasco-Soto, M.A., et al., Selective band gap manipulation of graphene oxide by its reduction with mild reagents. *Carbon*, 2015. **93**: pp. 967–973.
- [3] Huang, H., et al., Oxygen density dependent band gap of reduced graphene oxide. *Journal of Applied Physics*, 2012. **111**(5): p. 054317.
- [4] Hummers, W.S. and R.E. Offeman, Preparation of graphitic oxide. *Journal of the American Chemical Society*, 1958. **80**(6): pp. 1339–1339.
- [5] Velasco-Soto, M.A., et al., Chapter 8 - Carbon Polymer Nanocomposites A2 - Domínguez, M. Sánchez, in *Nanocolloids*, C.R. Abreu, Editor. 2016, Elsevier: Amsterdam. pp. 265–297.
- [6] Dreyer, D.R., et al., The chemistry of graphene oxide. *Chemical Society Reviews*, 2010. **39**(1): pp. 228–240.
- [7] Thompson, B.C. and J.M.J. Fréchet, Polymer–fullerene composite solar cells. *Angewandte Chemie International Edition*, 2008. **47**(1): pp. 58–77.
- [8] Green, M.A., et al., Solar cell efficiency tables (version 47). *Progress in Photovoltaics: Research and Applications*, 2016. **24**(1): pp. 3–11.
- [9] Xue, J., et al., A hybrid planar–mixed molecular heterojunction photovoltaic cell. *Advanced Materials*, 2005. **17**(1): pp. 66–71.
- [10] Yu, G., et al., Polymer photovoltaic cells: enhanced efficiencies via a network of internal donor-acceptor heterojunctions. *Science*, 1995. **270**(5243): pp. 1789–1791.
- [11] Krebs, F.C., *Polymer photovoltaics: a practical approach*. Vol. 175. 2008: SPIE Press Bellingham, WA.
- [12] Velasco-Soto, M.A., *Desarrollo de Celdas Solares Poliméricas Usando Derivados de Grafeno*. 2016, Centro de Investigación de Materiales Avanzados Unidad Monterrey: Apodoca N.L.
- [13] Moliton, A. and J.-M. Nunzi, How to model the behaviour of organic photovoltaic cells. *Polymer International*, 2006. **55**(6): pp. 583–600.
- [14] Brodie, B.C., On the atomic weight of graphite. *Philosophical Transactions of the Royal Society of London*, 1859. **149**: pp. 249–259.
- [15] Staudenmaier, L., Verfahren zur darstellung der graphitsäure. *Berichte der deutschen chemischen Gesellschaft*, 1898. **31**(2): pp. 1481–1487.
- [16] Shen, Y., et al., Evolution of the band-gap and optical properties of graphene oxide with controllable reduction level. *Carbon*, 2013. **62**: pp. 157–164.
- [17] Paredes, J.I., et al., Graphene oxide dispersions in organic solvents. *Langmuir*, 2008. **24**(19): pp. 10560–10564.

- [18] Qu, S., et al., Noncovalent functionalization of graphene attaching [6,6]-Phenyl-C61-butyric acid methyl ester (PCBM) and application as electron extraction layer of polymer solar cells. *ACS Nano*, 2013. **7**(5): pp. 4070–4081.
- [19] Bai, S., et al., Reversible phase transfer of graphene oxide and its use in the synthesis of graphene-based hybrid materials. *Carbon*, 2011. **49**(13): pp. 4563–4570.
- [20] Velasco-Soto, M. A., et al. Chapter 7 - Dispersion of Carbon Nanomaterials. pp 251 in *Nanocolloids: A Meeting Point for Scientists and Technologists*. Domínguez-Sánchez, M. and Rodríguez-Abreu, C. 2016. Amsterdam, Elsevier: 247–263.
- [21] Rani, P. and V.K. Jindal, Designing band gap of graphene by B and N dopant atoms. *RSC Advances*, 2013. **3**(3): pp. 802–812.
- [22] Novoselov, K.S., et al., Electric field effect in atomically thin carbon films. *Science*, 2004. **306**(5696): pp. 666–669.
- [23] Zheng, F., et al., Charge transfer from poly(3-hexylthiophene) to graphene oxide and reduced graphene oxide. *RSC Advances*, 2015. **5**(109): pp. 89515–89520.
- [24] Wang, Z., et al., Technology ready use of single layer graphene as a transparent electrode for hybrid photovoltaic devices. *Physica E: Low-dimensional Systems and Nanostructures*, 2011. **44**(2): pp. 521–524.
- [25] Chen, S., et al., A graphene oxide/oxygen deficient molybdenum oxide nanosheet bilayer as a hole transport layer for efficient polymer solar cells. *Journal of Materials Chemistry A*, 2015. **3**(36): pp. 18380–18383.
- [26] Jeon, Y.-J., et al., High-performance polymer solar cells with moderately reduced graphene oxide as an efficient hole transporting layer. *Solar Energy Materials and Solar Cells*, 2012. **105**: pp. 96–102.
- [27] Robaey, P., et al., Enhanced performance of polymer:fullerene bulk heterojunction solar cells upon graphene addition. *Applied Physics Letters*, 2014. **105**(8): p. 083306.
- [28] Wang, J., et al., Composition and annealing effects in solution-processable functionalized graphene oxide/P3HT based solar cells. *Synthetic Metals*, 2010. **160**(23–24): pp. 2494–2500.
- [29] Bernardi, M., et al., Nanocarbon-based photovoltaics. *ACS Nano*, 2012. **6**(10): pp. 8896–8903.
- [30] Chuang, M.-K., et al., Gold nanoparticle-decorated graphene oxides for plasmonic-enhanced polymer photovoltaic devices. *Nanoscale*, 2014. **6**(3): pp. 1573–1579.
- [31] Ou, C.F., The effect of graphene/Ag nanoparticles addition on the performances of organic solar cells. *Journal of Materials Science and Chemical Engineering*, 2015. **3**: pp. 30–35.
- [32] Sutradhar, P. and M. Saha, Silver nanoparticles: synthesis and its nanocomposites for heterojunction polymer solar cells. *The Journal of Physical Chemistry C*, 2016. **120**(16): pp. 8941–8949.